HHS Public Access

Author manuscript

J Biomech. Author manuscript; available in PMC 2022 December 02.

Published in final edited form as:

J Biomech. 2021 December 02; 129: 110771. doi:10.1016/j.jbiomech.2021.110771.

Mechanical Metrics May Show Improved Ability to Predict Osteoarthritis Compared to T1rho Mapping

Hattie C. Cutcliffe[1,2], **Pavan K. Kottamasu**[1], **Amy L. McNulty**[1,3], **Adam P. Goode**[1,4,5], **Charles E. Spritzer**[2,6], **Louis E. DeFrate**[*,1,2,7]

[1]Department of Orthopaedic Surgery, Duke University and Duke University School of Medicine, Durham, NC, 27708

[2]Department of Biomedical Engineering, Duke University and Duke University School of Medicine, Durham, NC, 27708

[3]Department of Pathology, Duke University and Duke University School of Medicine, Durham, NC, 27708

[4]Department of Population Health Sciences, Duke University and Duke University School of Medicine, Durham, NC, 27708

[5]Duke Clinical Research Institute, Duke University and Duke University School of Medicine, Durham, NC, 27708

[6]Department of Radiology, Duke University and Duke University School of Medicine, Durham, NC, 27708

[7]Department of Mechanical Engineering and Materials Science, Duke University and Duke University School of Medicine, Durham, NC, 27708

Abstract

Changes in cartilage structure and composition are commonly observed during the progression of osteoarthritis (OA). Importantly, quantitative magnetic resonance imaging (MRI) methods, such as T1rho relaxation imaging, can noninvasively provide *in vivo* metrics that reflect changes in cartilage composition and therefore have the potential for use in early OA detection. Changes in cartilage mechanical properties are also hallmarks of OA cartilage; thus, measurement of cartilage mechanical properties may also be beneficial for earlier OA detection. However, the relative predictive ability of compositional versus mechanical properties in detecting OA has yet to be determined. Therefore, we developed logistic regression models predicting OA status in an *ex vivo* environment using several mechanical and compositional metrics to assess which metrics most effectively predict OA status. Specifically, in this study the compositional metric analyzed was

[*]**Corresponding Author:** Louis E. DeFrate, Ph.D. Professor in Orthopaedic Surgery, Biomedical Engineering, and Mechanical, Engineering and Materials Science, Duke University and Duke University School of Medicine, Medical Sciences Research Building I, 203 Research Drive, Room 375, DUMC Box 3093, Durham, NC 27710, Phone: 919-681-9959, Fax: 919-681-8490, lou.defrate@duke.edu.

the T1rho relaxation time, while the mechanical metrics analyzed were the stiffness and recovery (defined as a measure of how quickly cartilage returns to its original shape after loading) of the cartilage. Cartilage recovery had the best predictive ability of OA status both alone and in a multivariate model including the T1rho relaxation time. These findings highlight the potential of cartilage recovery as a non-invasive marker of *in vivo* cartilage health and motivate future investigation of this metric clinically.

Keywords

cartilage stiffness; cartilage recovery; cartilage mechanical properties; quantitative MRI; biomarker; OA diagnosis

Introduction

Currently, the clinical diagnosis of osteoarthritis (OA) is based on both radiographic findings (such as joint space narrowing, a surrogate of cartilage loss) and pain (Glyn-Jones et al., 2015; Kellgren and Lawrence, 1957; Lawrence et al., 2008; Litwic et al., 2013). However, these features do not occur until advanced stages of OA (Litwic et al., 2013; Lorenz and Richter, 2006) when treatment is difficult. An advantage that magnetic resonance imaging (MRI) provides with regard to OA diagnosis is that MRI can visualize cartilage pathology directly before joint space narrowing can be assessed radiographically (Atkinson et al., 2019; Guermazi et al., 2015). Furthermore, changes in OA cartilage composition, such as decreased proteoglycan content, disrupted collagen architecture, and changes in hydration, have been shown to occur before visible changes in cartilage morphology (Hatcher et al., 2017; Hollander et al., 1995; Lorenz and Richter, 2006; Rivers et al., 2000; Thompson and Oegema, 1979). Quantitative MRI metrics reflect changes to *in vivo* cartilage composition and therefore may allow for even earlier detection of OA (Guermazi et al., 2015). Specifically, T1rho mapping is sensitive to the relative proteoglycan concentration in the tissue. Decreased T1rho relaxation times correlate with increased proteoglycan content (Collins et al., 2018a; Hatcher et al., 2017; Li et al., 2011), as well as with reduced water content due to exercise (Heckelman et al., 2020; Subburaj et al., 2012; Taylor et al., 2018). Importantly, these established quantitative MRI techniques reflect differences between control and OA subjects *in vivo* (Li et al., 2007; Stahl et al., 2009), and may have value as predictive indicators of OA (Atkinson et al., 2019).

OA is also associated with altered cartilage mechanical properties, including changes in cartilage thickness (Obeid et al., 1994; Roberts et al., 1986),stiffness (Armstrong and Mow, 1982; Bonassar et al., 1995; Grenier et al., 2014; Hatcher et al., 2017; Knecht et al., 2006; Rivers et al., 2000; Setton et al., 1994; Treppo et al., 2000; Wayne et al., 2003) and permeability (Bonassar et al., 1995; Grenier et al., 2014; Rivers et al., 2000; Setton et al., 1994; Wayne et al., 2003). Interestingly, recent animal studies have suggested that altered cartilage mechanical properties may reflect early cartilage degeneration that precedes OA-related changes measured using histological scoring systems (Collins et al., 2021; Doyran et al., 2017). These findings motivated our recent *in vivo* work (Cutcliffe et al., 2020) quantifying cartilage recovery (defined as a measure of how quickly the cartilage returns to

its original shape after loading) as a non-invasive means to measure cartilage mechanical properties. Specifically, since cartilage recovery depends on the stiffness, permeability, and thickness of the tissue (Cutcliffe et al., 2020; Cutcliffe and DeFrate, 2020), we developed a technique using MR imaging together with 3D modeling to non-invasively quantify *in vivo* cartilage recovery in response to exercise (Cutcliffe et al., 2020). However, the diagnostic ability (sensitivity, specificity, positive predictive value, negative predictive value) of mechanical metrics, such as cartilage recovery and cartilage stiffness, relative to that of compositional imaging metrics, such as T1rho mapping, remains to be determined.

Therefore, the purpose of this study was to examine the performance of cartilage recovery and cartilage stiffness relative to T1rho relaxation times and cartilage stiffness as predictors of cartilage OA status ex vivo, as a first step towards validating and comparing the use of these metrics *in vivo*. We hypothesized that mechanical metrics (stiffness and recovery) would show increased performance in predicting OA compared to T1rho relaxation times.

Methods

Sample Harvest and MRI

The overall data collection procedure is outlined in Figure 1. Intact knee joints (N = 8) were procured from skeletally mature female pigs after slaughter from a local abattoir. Tissue was only received from deceased animals who were not euthanized for the purposes of this study, so Institutional Animal Care and Use Committee (IACUC) approval was not required. Prior to dissection, each knee joint underwent MRI in the sagittal plane with the joint capsule intact using a 3 Tesla scanner (Trio Tim, Siemens, Erlangen, Germany) and an 8-channel knee coil (Invivo Corporation, Gainesville, FL) (Okafor et al., 2014). Two MR sequences were used for this study: a double-echo steady-state (DESS) sequence (field of view: 16 cm x 16 cm; matrix size: 512 px x 512 px; slice thickness: 1 mm; flip angle: 25°; repetition time: 17 ms; echo time: 6 ms; scan duration: ~10 min) and a T1rho map (field of view: 14 cm x 14 cm; matrix size: 256 px x 256 px; slice thickness: 3 mm; flip angle: 15°; repetition time: 3500 ms; echo time: 5.9 ms; spin-lock time: 5, 10, 40, 80 ms at 500 Hz; scan duration: ~13 min) (Collins et al., 2018a; Collins et al., 2018b; Okafor et al., 2014).

Next, joints were dissected to expose the femoral and tibial articular surfaces, from which 5 mm diameter cylindrical full-thickness cartilage explants were harvested. Explants were harvested across two sessions (one immediately after the pre-dissection imaging, and one after a single freeze/thaw cycle). Previous literature has shown that an additional freeze-thaw cycle does not alter measured *ex vivo* mechanical properties (Athanasiou et al., 1994; Athanasiou et al., 1991). Explants were removed from visually healthy cartilage regions, identified as a Collins grade of 0, and from visually degenerated cartilage regions (OA), identified as Collins grades of I or II (Collins and McElligott, 1960). Overall, n = 101 explants were harvested (n = 81 healthy, n = 20 OA) at different locations spanning the femoral and tibial surfaces. Explants were promptly wrapped in gauze soaked in phosphate-buffered saline (PBS) containing a protease inhibitor cocktail (Protease Inhibitor Cocktail Set I, Millipore Sigma) and stored at −20°C until mechanical testing. After harvest, each femur and tibia were MR imaged again, using only the DESS sequence (using the same parameters as listed above).

MRI Data Analysis

The post-dissection DESS MR images were used to identify the precise location of each explant within the T1rho images, as the cartilage defects resulting from explant harvest were visible on the post-dissection DESS images. This was accomplished by creating three-dimensional (3D) models from both the post-dissection DESS MR images and the pre-dissection T1rho images and registering them together. Creation of the 3D models involved manual segmentation of the boundaries of the tibial and femoral cortices in each MRI slice of the DESS and T1rho images using solid modeling software (Rhinoceros 4.0, Robert McNeel and Associates) (Figure 2). The cartilage defects were also segmented in every slice in which they appeared in the post-dissection DESS images. The segmentations were used to create 3D surface models (Geomagic Studio 11, 3D Systems). Then, the 3D surface models of the femur and tibia from the post-dissection DESS scan were registered separately to the corresponding surface model from the T1rho scan (Geomagic Studio 11). This procedure allowed for the pixels in the T1rho images within each explant to be identified and used for further analysis.

Subsequently, the mean T1rho relaxation time of each explant (Borthakur et al., 2003; Hatcher et al., 2017; Li et al., 2007) was calculated using custom software written in MATLAB (version R2018a, Mathworks) as follows: first, all tibial and femoral cartilage was manually segmented in each slice of the scan from the first acquired spin lock time. Then, these slice-specific segmentations were applied to the scans from subsequent spin lock times to denote the pixels comprising cartilage. For all cartilage pixels, the signal intensity was extracted from the scans of every spin lock time and fit with an exponential function (*Equation 1*) to quantify the relaxation time of each pixel (Li et al., 2007). Finally, the relaxation time of each explant was calculated as the mean relaxation time across all pixels within each explant, as identified from the post-dissection DESS MRI.

$$S = S_0 e^{\left(-\frac{t}{\tau}\right)} \quad \text{(Equation 1)}$$

where S = signal intensity, t = spin lock time, and τ = fitted T1rho relaxation time constant.

Mechanical Testing

Explants were thawed for 30 minutes at room temperature, after which 3 mm diameter cylindrical plugs were cut from the original 5 mm diameter explants. The 3 mm plugs were loaded into a confined compression fixture for mechanical testing, which was filled with PBS containing a protease inhibitor cocktail. An MTS Acumen 3 materials test system (MTS Systems Corporation) was used to carry out creep and recovery tests in load control, similar to our previous work (Cutcliffe and DeFrate, 2020).

The test protocol began with cyclic preconditioning (0.1 N to 0.3 N peak-to-peak compressive sinusoid cycling at 0.10 Hz for 200 cycles) to allow the plugs to reach a steady-state level of hydration. This number of loading cycles at this frequency forces fluid alternately out of and into the tissue, until it reaches a dynamic equilibrium where no additional ratcheting strain accumulates per cycle (Gao et al., 2015). Then, explants equilibrated to a baseline thickness under a 0.1 N compressive preload for 120 minutes

(Athanasiou et al., 1991; Mow et al., 1989). Next, a compressive load of 0.3 N was applied for 120 minutes so that plugs could reach creep equilibrium. This change in load (0.2 N) was chosen to result in less than 20% strain at the end of creep (Ateshian et al., 1997; Mow et al., 1989; Mow et al., 1980). Finally, a compressive recovery load of 0.1 N was applied for 120 minutes. The rate at which the preload, creep, and recovery loads were applied was 0.05 N/s.

Mechanical Testing Data Analysis

The deformation response of both creep and recovery was fit with the biphasic solution corresponding to confined compression creep (Mow et al., 1980) (*Equation 2)* to quantify the aggregate modulus of the creep phase (H_A) and the characteristic time constant of the recovery phase (τ_0(Armstrong and Mow, 1982)), as in our previous work (Cutcliffe and DeFrate, 2020). The aggregate modulus of the creep phase is subsequently referred to as “stiffness”, while the characteristic time constant of the recovery phase is subsequently referred to as “recovery”. Nonlinear least-squares curve-fitting was implemented in MATLAB to fit the theoretical solution to the experimental data. Baseline thickness was calculated as the average explant thickness over the last five minutes of the preload application (Cutcliffe and DeFrate, 2020).

$$\frac{u}{h} = -\frac{\sigma_0}{H_A}\left[1 - 2\sum_{n=0}^{\infty}\frac{1}{\pi^2\left(n+\frac{1}{2}\right)}e^{-\pi^2\left(n+\frac{1}{2}\right)^2\frac{t}{\tau}}\right] \quad \text{(Equation 2a)}$$

$$\tau = \frac{h^2}{H_A k} \quad \text{(Equation 2b)}$$

$$\tau_0 = \frac{4}{\pi^2}\tau = \frac{4h^2}{\pi^2 H_A k} \quad \text{(Equation 2c)}$$

where u = surface displacement; h = baseline thickness; σ_0 = applied compressive stress; H_A = aggregate modulus; k = permeability; τ = time constant; t = time; τ_0 = characteristic time constant.

Statistical Analysis

Statistical modeling was carried out using SAS (SAS 9.4, SAS Institute Inc.) with $p < 0.05$ indicating statistical significance. As stated, the goal of the current study was to predict the presence or absence of OA as a function of mechanical and compositional metrics (stiffness, recovery, and T1rho relaxation times). Each of these three metrics were continuous variables.

To determine if differences existed in each of the three metrics (stiffness, recovery, and T1rho relaxation time) between healthy and OA explants, a two-way ANOVA was performed. In this ANOVA, the two factors were bone surface (femur vs tibia, the surface where each cartilage explant was harvested) and OA status (healthy vs OA).

Next, logistic regression was used to determine the association between cartilage OA status (where the presence of OA was coded as 1 and the absence of OA (healthy) was coded as 0) and the three metrics. Initially, we modeled the bivariate relationship between OA status and each of the three metrics individually. Then, we modeled the multivariate relationship between OA status and all three of the metrics together. We assessed the performance of each logistic regression model using model properties (sensitivity, specificity) and performance characteristics (positive predictive value (PPV), negative predictive value (NPV), area under the receiver operating characteristic curve (AUC)), along with 95% confidence intervals of each property or characteristic as a measure of the variability. A 0.5 was added to each cell with a count of zero in the 2×2 tables for the purposes of calculating model performance characteristics (Haldane, 1940).

Results

Overall summary statistics (mean ± 95% confidence intervals) are presented in Table 1. OA explants displayed significantly longer recovery and lower stiffness than healthy explants (Figure 3). OA explants also showed significantly increased T1rho relaxation times. A significant main effect of bone surface (femur vs tibia) was found for stiffness, with tibial samples having significantly higher stiffness than femoral samples. No main effect of bone surface on the recovery or T1rho relaxation time was detected.

To investigate the ability of the three metrics to predict OA, bivariate logistic regression modeling was performed. A description of the three bivariate models is presented in Table 2 and a plot of each model is given in Figure 4. Recovery, stiffness, and T1rho relaxation time were each significantly associated with OA status in the bivariate models. However, the model using recovery demonstrated the largest per-unit change in odds with an 11% increased odds of OA for every 1 minute increase in recovery.

When these three metrics were used in a single multivariate model, recovery and T1rho relaxation time but not stiffness were found to be significantly associated with OA status (Table 3). As a result, a second parsimonious multivariate model (Table 3) was performed, which included only the significant metrics (recovery and T1rho relaxation times). In this parsimonious multivariate model, each included metric was found to be significantly associated with OA status, and again the recovery showed the largest per-unit change in odds of OA (11% increased odds of OA).

Table 4 contains the model properties and performance characteristics, while graphs of the receiver operating characteristic curves are given in Figure 5. The bivariate models using mechanical metrics showed improved ability in predicting OA (better model properties and performance characteristics) compared to the bivariate model using the compositional imaging metric (T1rho relaxation time). Specifically, the bivariate model using recovery showed the best overall ability to predict OA, as it demonstrated the highest value in all three performance characteristics (PPV, NPV, and AUC), the highest value in one of the two model properties (sensitivity), and the second-highest value in the other model property (specificity). In fact, the bivariate model using recovery illustrated a similar predictive capacity as the parsimonious multivariate model: it resulted in an identical 2×2 table and

demonstrated equal model properties (sensitivity and specificity) and equal values in two of the three performance characteristics (PPV and NPV).

Discussion

Clinical diagnosis of OA requires the presence of pain and radiographic findings (Glyn-Jones et al., 2015; Kellgren and Lawrence, 1957; Lawrence et al., 2008; Litwic et al., 2013), which are features of advanced OA (Litwic et al., 2013; Lorenz and Richter, 2006). The detection of cartilage pathology using changes in mechanical response (Chan et al., 2016; Coleman et al., 2013; Eckstein et al., 2005; Eckstein et al., 1999; Eckstein et al., 1998; Lad et al., 2016; Paranjape et al., 2019) and quantitative MRI measures of composition (Collins et al., 2018a; Hatcher et al., 2017; Knecht et al., 2006; Li et al., 2007; Stahl et al., 2009) may allow for earlier diagnosis and possibly more efficacious therapeutic techniques. However, the predictive value of mechanical and quantitative MRI metrics in identifying OA cartilage has not been assessed. Therefore, the goal of this study was to investigate the ability of mechanical and compositional imaging metrics to predict OA status *ex vivo* in order to explore and validate their potential future use as predictive or diagnostic indicators *in vivo*.

Overall, we found that mechanical metrics predicted *ex vivo* OA status more effectively than did the compositional imaging metric. Specifically, the model using cartilage recovery — a structural mechanical property related to the tissue's stiffness, permeability, and thickness (Armstrong and Mow, 1982; Mow et al., 1980) — demonstrated the best performance out of the three bivariate models (Table 4, Figure 5). This illustrates that cartilage recovery more accurately discriminated between OA and healthy explants than did the stiffness or T1rho relaxation time. Furthermore, the bivariate model using recovery showed a similar performance compared with the parsimonious multivariate model incorporating both the recovery and T1rho relaxation time (Table 4, Figure 5). This result suggests minimal additional benefit of including T1rho relaxation time in models including cartilage recovery for the purposes of OA prediction.

Likewise, in the original multivariate model incorporating all three metrics, the stiffness was not significantly associated with OA status, despite it being significantly associated with OA status in the bivariate model. Prior work has shown stiffness to be significantly correlated with recovery (Cutcliffe and DeFrate, 2020). This suggests that in models including recovery, the stiffness contributes mostly redundant information about the mechanical state of the cartilage. Furthermore, while cartilage recovery has been previously measured *in vivo*, (Cutcliffe et al., 2020) measurement of cartilage stiffness *in vivo* remains challenging. Taken together, these results motivate further investigation of cartilage recovery as a potential stand-alone *in vivo* indicator of OA.

Overall, our results illustrate that changes in cartilage health may be more accurately identified via measurement of mechanical properties (cartilage recovery and stiffness) than through measurement of composition via quantitative MRI (T1rho relaxation time). Nonetheless, baseline quantitative MRI may provide important information about cartilage composition and health, especially in early OA (Atkinson et al., 2019). Some studies (Collins et al., 2018a; Hatcher et al., 2017; Tang et al., 2011) have observed changes in

mechanical properties concomitant with changes in T1rho relaxation times, as in the present study. Yet, it remains unclear whether quantitative imaging findings or mechanical changes were more effective indicators of OA status. Towards this end, our results demonstrate that while quantitative imaging metrics show significant differences between healthy and OA cartilage, they are less effective predictors of OA than mechanical properties (such as the stiffness and recovery). In further support of this hypothesis, a recent study modeling OA in mice through surgical destabilization of the medial meniscus (Doyran et al., 2017) found that significant decreases in stiffness were evident within a week after surgery, while histological markers of OA (e.g., cartilage thinning and/or fibrillation, changes in proteoglycan staining) were not apparent until 4 weeks after surgery, suggesting that mechanical properties may be sensitive to some of the earliest changes in cartilage health. As recovery is a mechanical property of cartilage, it may also represent a useful, non-invasive MRI metric (Cutcliffe et al., 2020) that is sensitive to early changes in cartilage health.

It should be noted that our analysis took place in the *ex vivo* environment in order to verify the presence or absence of cartilage degeneration. As a result, the mechanical metrics in this study were measured using *ex vivo* mechanical testing. Nonetheless, cartilage recovery times measured in the present study (~27 min) were comparable to that measured *in vivo* in humans (~25 min) (Cutcliffe et al., 2020). Furthermore, while current MRI methods enable measurement of cartilage recovery *in vivo*, (Cutcliffe et al., 2020) determination of cartilage stiffness *in vivo* via MRI remains challenging. Additionally, we determined OA status using Collins grading (Collins and McElligott, 1960). Variability in mechanical and imaging measures were increased in OA samples compared to healthy samples (Table 1), which may be due to variations in Collins score. Despite this, we detected statistically significant differences in mechanical and imaging measures between our healthy and OA samples. Finally, due to the nature of our *ex vivo* testing, other important variables that influence the development of OA (such as age, obesity, or prior joint injury) were not available, so the models presented here were not adjusted for these factors. Therefore, the results of our study represent an *ex vivo* validation of the potential of cartilage recovery as a diagnostic marker of OA, and future studies investigating the clinical utility of this metric *in vivo* are needed.

Overall, the results of this study illustrate that cartilage recovery—a mechanical property that can be quantified non-invasively *in vivo* using MRI (Cutcliffe et al., 2020)—is predictive of cartilage OA status in the *ex vivo* environment. Importantly, cartilage recovery is a single property incorporating multiple aspects of mechanical function (thickness, stiffness, and permeability). As each of these aspects may change early in OA, (Knecht et al., 2006; Setton et al., 1994) possibly before other degenerative changes are visible (Doyran et al., 2017), cartilage recovery may prove to be a valuable indicator of early cartilage degeneration.

Acknowledgements

The authors would like to thank the Center for Advanced Magnetic Resonance Development at Duke University for their assistance with this project and would like to gratefully acknowledge Lia Meirose for her helpful discussions concerning this study. The authors acknowledge the assistance of Donald T. Kirkendall, PhD, ELS for his help

is preparing this paper for submission. This study was supported by the NIH grants AR065527, AR074800, AR073221, AR079184, and AR075399.

Bibliography

Armstrong C, Mow V, 1982. Variations in the intrinsic mechanical properties of human articular cartilage with age, degeneration, and water content. J Bone Joint Surg Am 64, 88–94. [PubMed: 7054208]

Ateshian G, Warden W, Kim J, Grelsamer R, Mow V, 1997. Finite deformation biphasic material properties of bovine articular cartilage from confined compression experiments. Journal of Biomechanics 30, 1157–1164. [PubMed: 9456384]

Athanasiou K, Agarwal A, Dzida F, 1994. Comparative study of the intrinsic mechanical properties of the human acetabular and femoral head cartilage. Journal of Orthopaedic Research 12, 340–349. [PubMed: 8207587]

Athanasiou K, Rosenwasser M, Buckwalter J, Malinin T, Mow V, 1991. Interspecies comparisons of in situ intrinsic mechanical properties of distal femoral cartilage. Journal of Orthopaedic Research 9, 330–340. [PubMed: 2010837]

Atkinson HF, Birmingham TB, Moyer RF, Yacoub D, Kanko LE, Bryant DM, Thiessen JD, Thompson RT, 2019. MRI T2 and T1ρ relaxation in patients at risk for knee osteoarthritis: a systematic review and meta-analysis. BMC musculoskeletal disorders 20, 182. [PubMed: 31039785]

Bonassar LJ, Frank EH, Murray JC, Paguio CG, Moore VL, Lark MW, Sandy JD, Wu JJ, Eyre DR, Grodzinsky AJ, 1995. Changes in cartilage composition and physical properties due to stromelysin degradation. Arthritis & Rheumatism: Official Journal of the American College of Rheumatology 38, 173–183.

Borthakur A, Wheaton A, Charagundla SR, Shapiro EM, Regatte RR, Akella SV, Kneeland JB, Reddy R, 2003. Three-dimensional T1ρ-weighted MRI at 1.5 Tesla. Journal of Magnetic Resonance Imaging 17, 730–736. [PubMed: 12766904]

Chan DD, Cai L, Butz KD, Trippel SB, Nauman EA, Neu CP, 2016. In vivo articular cartilage deformation: noninvasive quantification of intratissue strain during joint contact in the human knee. Scientific reports 6, 19220. [PubMed: 26752228]

Coleman JL, Widmyer MR, Leddy HA, Utturkar GM, Spritzer CE, Moorman CT, Guilak F, DeFrate LE, 2013. Diurnal variations in articular cartilage thickness and strain in the human knee. Journal of Biomechanics 46, 541–547. [PubMed: 23102493]

Collins AT, Hatcher C, Kim S, Ziemian S, Spritzer C, Guilak F, DeFrate L, McNulty A, 2018a. Selective enzymatic digestion of proteoglycans and collagens alters cartilage T1rho and T2 relaxation times. Annals of biomedical engineering, 1–12.

Collins AT, Hu G, Newman H, Reinsvold MH, Goldsmith MR, Twomey-Kozak JN, Leddy HA, Sharma D, Shen L, DeFrate LE, Karner CM, 2021. Obesity alters the collagen organization and mechanical properties of murine cartilage. Sci Rep 11, 1626. [PubMed: 33452305]

Collins AT, Kulvaranon ML, Cutcliffe HC, Utturkar GM, Smith WA, Spritzer CE, Guilak F, DeFrate LE, 2018b. Obesity alters the in vivo mechanical response and biochemical properties of cartilage as measured by MRI. Arthritis Research & Therapy 20, 232. [PubMed: 30333058]

Collins D, McElligott T, 1960. Sulphate (35SO4) uptake by chondrocytes in relation to histological changes in osteo-arthritic human articular cartilage. Annals of the rheumatic diseases 19, 318. [PubMed: 13694746]

Cutcliffe HC, Davis KM, Spritzer CE, DeFrate L, 2020. The Characteristic Recovery Time as a Novel, Noninvasive Metric for Assessing In Vivo Cartilage Mechanical Function. Ann Biomed Eng 48, 2901–2910. [PubMed: 32666421]

Cutcliffe HC, DeFrate LE, 2020. Comparison of Cartilage Mechanical Properties Measured During Creep and Recovery. Scientific Reports 10, 1–8. [PubMed: 31913322]

Doyran B, Tong W, Li Q, Jia H, Zhang X, Chen C, Enomoto-Iwamoto M, Lu XL, Qin L, Han L, 2017. Nanoindentation modulus of murine cartilage: a sensitive indicator of the initiation and progression of post-traumatic osteoarthritis. Osteoarthritis and cartilage 25, 108–117. [PubMed: 27568574]

Eckstein F, Lemberger B, Gratzke C, Hudelmaier M, Glaser C, Englmeier K, Reiser M, 2005. In vivo cartilage deformation after different types of activity and its dependence on physical training status. Annals of the Rheumatic Diseases 64, 291–295. [PubMed: 15647438]

Eckstein F, Tieschky M, Faber S, Englmeier K-H, Reiser M, 1999. Functional analysis of articular cartilage deformation, recovery, and fluid flow following dynamic exercise in vivo. Anatomy and Embryology 200, 419–424. [PubMed: 10460479]

Eckstein F, Tieschky M, Faber SC, Haubner M, Kolem H, Englmeier K-H, Reiser M, 1998. Effect of physical exercise on cartilage volume and thickness in vivo: MR imaging study. Radiology 207, 243–248. [PubMed: 9530322]

Gao L-L, Qin X-Y, Zhang C-Q, Gao H, Ge H-Y, Zhang X-Z, 2015. Ratcheting behavior of articular cartilage under cyclic unconfined compression. Materials Science and Engineering: C 57, 371–377.

Glyn-Jones S, Palmer A, Agricola R, Price A, Vincent T, Weinans H, Carr A, 2015. Osteoarthritis. The Lancet 386, 376–387.

Grenier S, Bhargava MM, Torzilli PA, 2014. An in vitro model for the pathological degradation of articular cartilage in osteoarthritis. Journal of Biomechanics 47, 645–652. [PubMed: 24360770]

Guermazi A, Alizai H, Crema M, Trattnig S, Regatte R, Roemer F, 2015. Compositional MRI techniques for evaluation of cartilage degeneration in osteoarthritis. Osteoarthritis and cartilage 23, 1639–1653. [PubMed: 26050864]

Haldane J, 1940. The Mean and Variance of| chi 2, When Used as a Test of Homogeneity, When Expectations are Small. Biometrika 31, 346–355.

Hatcher CC, Collins AT, Kim SY, Michel LC, Mostertz WC, Ziemian SN, Spritzer CE, Guilak F, DeFrate LE, McNulty AL, 2017. Relationship between T1rho magnetic resonance imaging, synovial fluid biomarkers, and the biochemical and biomechanical properties of cartilage. Journal of Biomechanics 55, 18–26. [PubMed: 28237185]

Heckelman LN, Smith WA, Riofrio AD, Vinson EN, Collins AT, Gwynn OR, Utturkar GM, Goode AP, Spritzer CE, DeFrate LE, 2020. Quantifying the biochemical state of knee cartilage in response to running using T1rho magnetic resonance imaging. Scientific Reports 10, 1–7. [PubMed: 31913322]

Hollander A, Pidoux I, Reiner A, Rorabeck C, Bourne R, Poole AR, 1995. Damage to type II collagen in aging and osteoarthritis starts at the articular surface, originates around chondrocytes, and extends into the cartilage with progressive degeneration. Journal of Clinical Investigation 96, 2859.

Kellgren J, Lawrence J, 1957. Radiological assessment of osteo-arthrosis. Annals of the Rheumatic Diseases 16, 494. [PubMed: 13498604]

Knecht S, Vanwanseele B, Stüssi E, 2006. A review on the mechanical quality of articular cartilage–implications for the diagnosis of osteoarthritis. Clinical biomechanics 21, 999–1012. [PubMed: 16979270]

Lad NK, Liu B, Ganapathy PK, Utturkar GM, Sutter EG, Moorman CT 3rd, Garrett WE, Spritzer CE, DeFrate LE, 2016. Effect of normal gait on in vivo tibiofemoral cartilage strains. Journal of Biomechanics 49, 2870–2876. [PubMed: 27421206]

Lawrence RC, Felson DT, Helmick CG, Arnold LM, Choi H, Deyo RA, Gabriel S, Hirsch R, Hochberg MC, Hunder GG, 2008. Estimates of the prevalence of arthritis and other rheumatic conditions in the United States: Part II. Arthritis & Rheumatism 58, 26–35. [PubMed: 18163497]

Li X, Cheng J, Lin K, Saadat E, Bolbos RI, Jobke B, Ries MD, Horvai A, Link TM, Majumdar S, 2011. Quantitative MRI using T1ρ and T2 in human osteoarthritic cartilage specimens: correlation with biochemical measurements and histology. Magnetic resonance imaging 29, 324–334. [PubMed: 21130590]

Li X, Ma B, Thomas L, Castillo D, Blumenkrantz G, Lozano J, Carballido-Gamio J, Ries M, Majumdar S, 2007. In vivo T1Rho and T2 mapping of articular cartilage in osteoarthritis of the knee using 3 tesla MRI. Osteoarthritis Cartilage 15, 789–797. [PubMed: 17307365]

Litwic A, Edwards MH, Dennison EM, Cooper C, 2013. Epidemiology and burden of osteoarthritis. British medical bulletin 105, 185–199. [PubMed: 23337796]

Lorenz H, Richter W, 2006. Osteoarthritis: cellular and molecular changes in degenerating cartilage. Progress in Histochemistry and Cytochemistry 40, 135–163. [PubMed: 16759941]

Mow VC, Gibbs M, Lai WM, Zhu W, Athanasiou KA, 1989. Biphasic indentation of articular cartilage—II. A numerical algorithm and an experimental study. Journal of Biomechanics 22, 853–861. [PubMed: 2613721]

Mow VC, Kuei S, Lai WM, Armstrong CG, 1980. Biphasic creep and stress relaxation of articular cartilage in compression: theory and experiments. Journal of Biomechanical Engineering 102, 73–84. [PubMed: 7382457]

Obeid E, Adams M, Newman J, 1994. Mechanical properties of articular cartilage in knees with unicompartmental osteoarthritis. The Journal of bone and joint surgery British volume 76, 315–319. [PubMed: 8113301]

Okafor EC, Utturkar GM, Widmyer MR, Abebe ES, Collins AT, Taylor DC, Spritzer CE, Moorman C 3rd, Garrett WE, DeFrate LE, 2014. The effects of femoral graft placement on cartilage thickness after anterior cruciate ligament reconstruction. Journal of Biomechanics 47, 96–101. [PubMed: 24210473]

Paranjape CS, Cutcliffe HC, Grambow SC, Utturkar GM, Collins AT, Garrett WE, Spritzer CE, DeFrate LE, 2019. A New Stress Test for Knee Joint Cartilage. Scientific Reports 9, 2283. [PubMed: 30783146]

Rivers P, Rosenwasser M, Mow V, Pawluk R, Strauch R, Sugalski M, Ateshian G, 2000. Osteoarthritic changes in the biochemical composition of thumb carpometacarpal joint cartilage and correlation with biomechanical properties. Journal of Hand Surgery 25, 889–898.

Roberts S, Weightman B, Urban J, Chappell D, 1986. Mechanical and biochemical properties of human articular cartilage in osteoarthritic femoral heads and in autopsy specimens. The Journal of bone and joint surgery British volume 68, 278–288. [PubMed: 3958016]

Setton LA, Mow VC, Muller FJ, Pita JC, Howell DS, 1994. Mechanical properties of canine articular cartilage are significantly altered following transection of the anterior cruciate ligament. J Orthop Res 12, 451–463. [PubMed: 8064477]

Stahl R, Luke A, Li X, Carballido-Gamio J, Ma CB, Majumdar S, Link TM, 2009. T1rho, T 2 and focal knee cartilage abnormalities in physically active and sedentary healthy subjects versus early OA patients—a 3.0-Tesla MRI study. European radiology 19, 132–143. [PubMed: 18709373]

Subburaj K, Kumar D, Souza RB, Alizai H, Li X, Link TM, Majumdar S, 2012. The acute effect of running on knee articular cartilage and meniscus magnetic resonance relaxation times in young healthy adults. The American journal of sports medicine 40, 2134–2141. [PubMed: 22729505]

Tang SY, Souza RB, Ries M, Hansma PK, Alliston T, Li X, 2011. Local tissue properties of human osteoarthritic cartilage correlate with magnetic resonance T1rho relaxation times. Journal of orthopaedic research 29, 1312–1319. [PubMed: 21445940]

Taylor KA, Collins AT, Heckelman LN, Kim SY, Utturkar GM, Spritzer CE, Garrett WE, DeFrate LE, 2018. Activities of daily living influence tibial cartilage T1rho relaxation times. Journal of biomechanics 82, 228–233. [PubMed: 30455059]

Thompson R, Oegema T, 1979. Metabolic activity of articular cartilage in osteoarthritis. An in vitro study. J Bone Joint Surg Am 61, 407–416. [PubMed: 429413]

Treppo S, Koepp H, Quan EC, Cole AA, Kuettner KE, Grodzinsky AJ, 2000. Comparison of biomechanical and biochemical properties of cartilage from human knee and ankle pairs. Journal of Orthopaedic Research 18, 739–748. [PubMed: 11117295]

Wayne JS, Kraft KA, Shields KJ, Yin C, Owen JR, Disler DG, 2003. MR imaging of normal and matrix-depleted cartilage: correlation with biomechanical function and biochemical composition. Radiology 228, 493–499. [PubMed: 12893905]

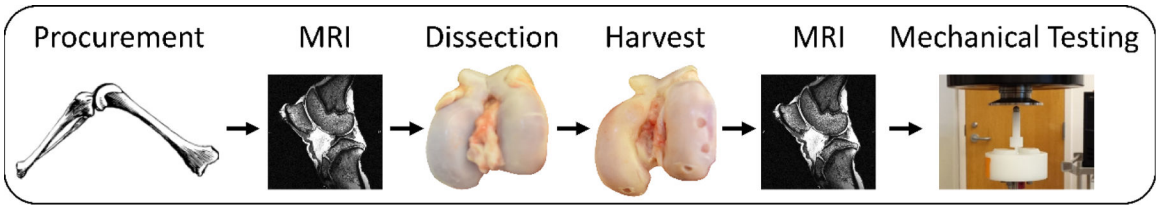

Figure 1:
Overall data collection procedure. Joints were procured, MR imaged, dissected, cartilage explants were harvested, and then MR imaged again. Subsequently, cartilage explants were mechanically tested.

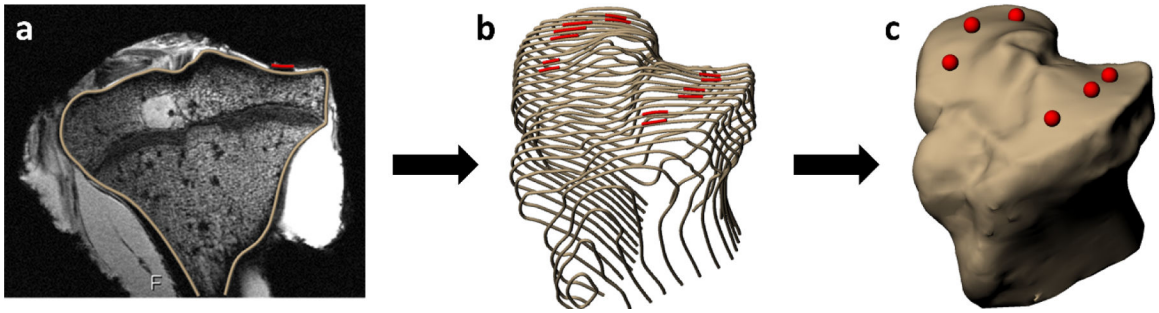

Figure 2:
Cartilage defect (red) measurement procedure, showing a) segmentation of the tibial cortex and tibial articular cartilage explant harvest sites, b) compilation of segmentations across several slices, and c) 3D surface mesh model creation.

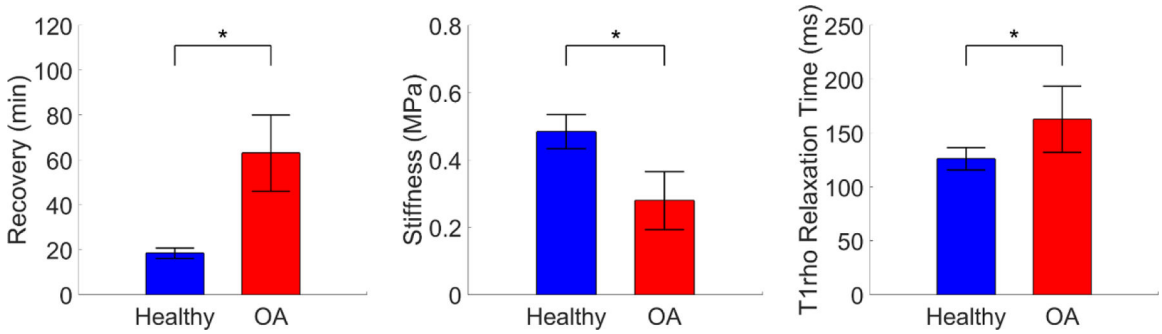

Figure 3:

Differences across OA status in each continuous metric. Error bars represent 95% confidence intervals. *Significant main effect of OA status, $p < 0.05$.

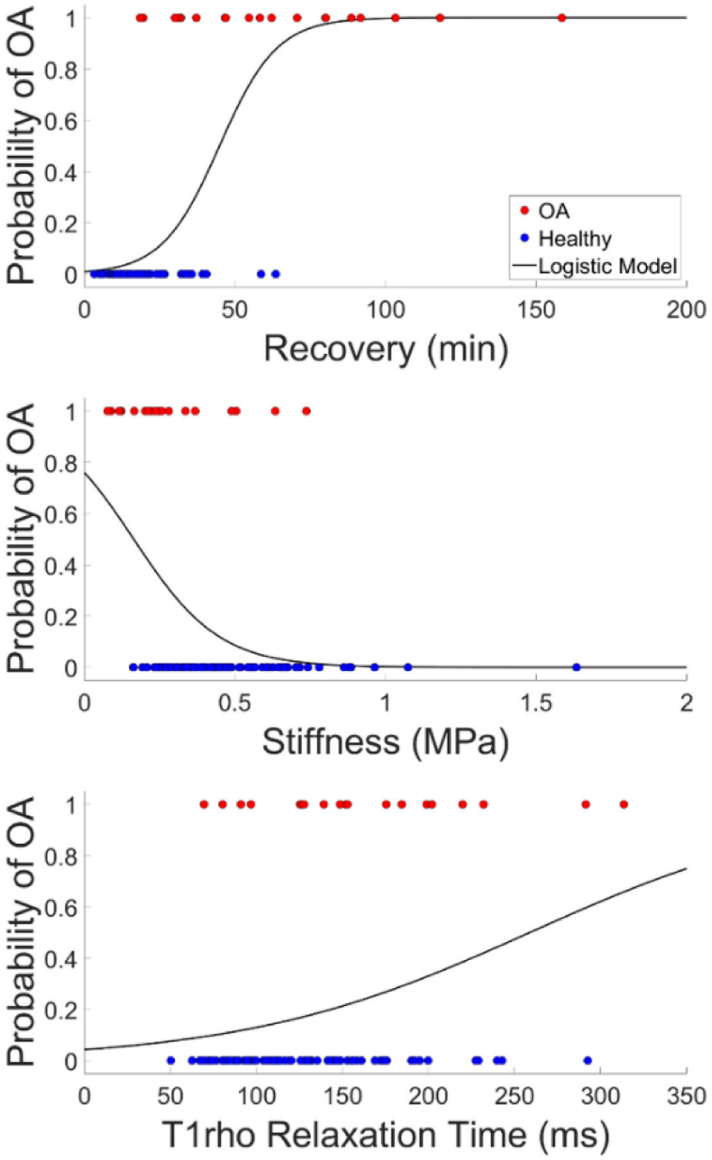

Figure 4:
Bivariate logistic regression models of the probability of OA (where 1 = OA, 0 = healthy) based on each of the three continuous metrics.

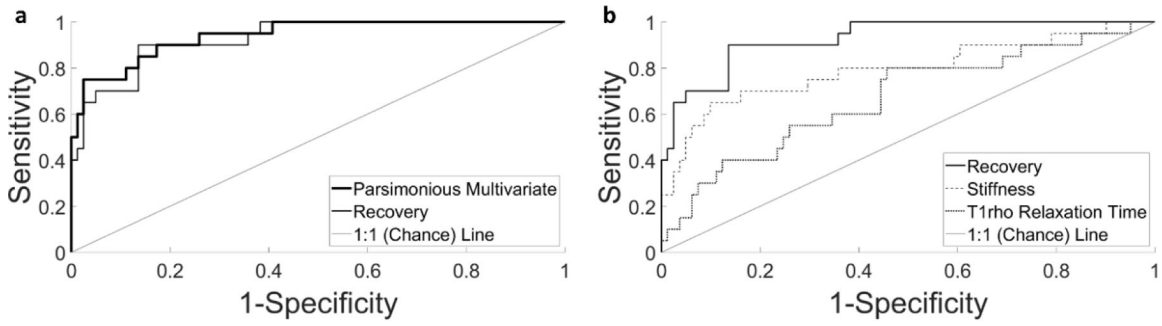

Figure 5:

Receiver operating characteristic curves for the parsimonious multivariate and bivariate models, representing the relationship between the true positive proportion and the false positive proportion for predicting OA status. A) Comparison of the parsimonious multivariate model and the bivariate model using the recovery. B) Comparison of all three bivariate models.

Table 1:

Summary statistics for cartilage explant dataset

	Total (Healthy & OA) Mean (± 95% CI)	Healthy Tibia Mean (± 95% CI)	Healthy Femur Mean (± 95% CI)	OA Tibia Mean (± 95% CI)	OA Femur Mean (± 95% CI)
Sample size (n)	101	49	32	8	12
Recovery (min)	27.3 (5.1)	17.4 (3.0)	20.0 (3.9)	72.5 (43.3)	56.7 (13.7)
Stiffness (MPa)	0.44 (0.05)	0.54 (0.07)	0.41 (0.07)	0.39 (0.20)	0.20(0.05)
T1rho Relaxation Time (ms)	133.3 (10.4)	127.5 (13.3)	123.8 (17.6)	131.0 (28.6)	183.8 (47.1)

CI = confidence interval.

Table 2:

Description of bivariate logistic regression models

Predictor Included in Model	Intercept (± Standard Error)	Parameter Estimate (± Standard Error)	P=	Odds Ratio (95% Wald Confidence Limits)
Recovery (min)	−4.72 (0.84)	0.11 (0.02)	<0.0001	1.11 (1.06, 1.17)
Stiffness (Pa)	1.15 (0.69)	-7.03×10^{-6} (2.04×10^{-6})	0.0006	1.00 (1.00, 1.00)
T1rho Relaxation Time (ms)	−3.11 (0.74)	0.01 (0.00)	0.0090	1.01 (1.00, 1.02)

Table 3:

Description of multivariate logistic regression models

Predictor	Parameter Estimate (± Standard Error)	P =	Odds Ratio (95% Wald Confidence Limits)
	Complete Model		
Intercept	−6.57 (1.93)	0.0007	---
Recovery (min)	0.10 (0.03)	0.0003	1.11 (1.05, 1.17)
Stiffness (Pa)	-4.00×10^{-7} (2.11×10^{-6})	0.8497	1.00 (1.00, 1.00)
T1rho Relaxation Time (ms)	0.01 (0.01)	0.0395	1.01 (1.00, 1.03)
	Parsimonious Model		
Intercept	−6.81 (1.49)	<0.0001	---
Recovery (min)	0.11 (0.03)	<0.0001	1.11 (1.06, 1.17)
T1rho Relaxation Time (ms)	0.01 (0.01)	0.0390	1.01 (1.00, 1.03)

Table 4:

Property and performance characteristics of logistic regression models

Model	Sensitivity (± 95% CI)	Specificity (± 95% CI)	PPV (± 95% CI)	NPV (± 95% CI)	AUC
Parsimonious Multivariate	0.65 (0.41, 0.85)	0.98 (0.91, 1.00)	0.87 (0.60, 0.98)	0.92 (0.84, 0.97)	0.94
Bivariate, Recovery	0.65 (0.41, 0.85)	0.98 (0.91, 1.00)	0.87 (0.60, 0.98)	0.92 (0.84, 0.97)	0.93
Bivariate, Stiffness	0.25 (0.09, 0.49)	0.98 (0.91, 1.00)	0.71 (0.29, 0.96)	0.84 (0.75, 0.91)	0.79
Bivariate, T1rho Relaxation Time	0.10 (0.01, 0.32)	0.99 (0.93, 1.00)	0.67 (0.09, 0.99)	0.82 (0.73, 0.89)	0.67

CI = confidence interval, PPV = positive predictive value, NPV = negative predictive value, AUC = area under the receiver operating characteristic curve.